# Wall Heat Fluxes in Rocket Combustion Chamber with Porous Injector Head

*Victor P. Zhukov and Dmitry I. Suslov*
*Institute of Space Propulsion, German Aerospace Center (DLR)*
*Langer Grund, 74239 Hardthausen, Germany*

## Abstract

Wall heat fluxes in a rocket combustion chamber with a porous injector head are measured by the calorimetric method at the ratio of oxidizer to fuel of 6 and pressure of 80 bars. The flow inside the combustion chamber is simulated using the commercial CFD code ANSYS CFX. Turbulence is modelled by the Favre averaged Navier-Stokes equations and the Shear-Stress-Transport model. The turbulent combustion of propellants is modelled using different models: the Eddy Dissipation Model and the Extended Coherent Flame Model. The results obtained with the different models are compared. The numerical results agree with the experimental results well.

## 1. Introduction

The usage of porous materials can improve performance of rocket combustion chamber. The application of porous injector head can provide the effective mixing of fuel and oxidizer at low pressure drop in the injector head. This new injection concept is currently under development at the German Aerospace Center (DLR-Lampoldshausen) [1-3]. Nowadays the porous injector faceplates are used in some rocket engines (for example: SSME and J-2) where the small part of the fuel flow is fed through the porous injector faceplate in order to cool it and the main part of the fuel is still injected through coaxial injectors [4]. Coaxial injectors proved their efficiency, but they require the very precise manufacture and keep their efficiency in the narrow range of mass flows which is limited from above and below. These problems can be easily solved by the application of porous injector head. According to the hot-tests at DLR-Lampoldshausen [2] the porous injector head (Fig. 1) allows to maintain the high combustion efficiency over the wide throttling range from 37.5% to 125%. Besides the manufacture costs and the throttling capability porous injector head has two additional advantages over conventional coaxial injectors. Porous injector head operates at a smaller pressure drop than the injector head with coaxial injectors. The small diameter of the injectors in a porous head results in the small jet break-up distance which allows reducing the length of chamber. Such features improve the performance of rocket engines.

Rocket combustion chambers are exposed under severe thermal loads during the burn. The components of a thrust chamber assembly: injector head, side walls, and nozzle require the adequate cooling. The proper design of a rocket combustion chamber needs the knowledge about the heat fluxes inside the chamber. There is the accumulated experience of experimental tests and simulations of the conventional injectors (impinging and co-axial) while the existed knowledge on porous injector head is not enough.

Zhukov and Haidn [5] considered the heat transfer in a porous injector plate at the conditions of the current work. They found an analytical expression connecting the incident heat flux and the temperature of the hot side wall of a porous injector head. It was shown that the heat loads are not problematic at least for an injector head made from sintered bronze (i.e. for the injector head which is used in the current work). However, the thermal loads are still an issue for other parts of thrust chamber assembly.

While the wall heat flux reaches a maximum in the throat of combustion chamber, the peculiarities of injector head should be negligible there and further downstream in the nozzle (the flow in a “good” combustion chamber should be enough uniform in the throat). The particularities of porous injector head should come out at the first 100 mm from the injector plate. Here the parameters of the flow depend strongly on the injection conditions. The flow and the heat fluxes in a combustion chamber with coaxial injectors were studied extensively in the series of works from Astrium [6-8] (and also by many other researchers). However, the numerical analysis of the flame of porous injector head has not been done yet.

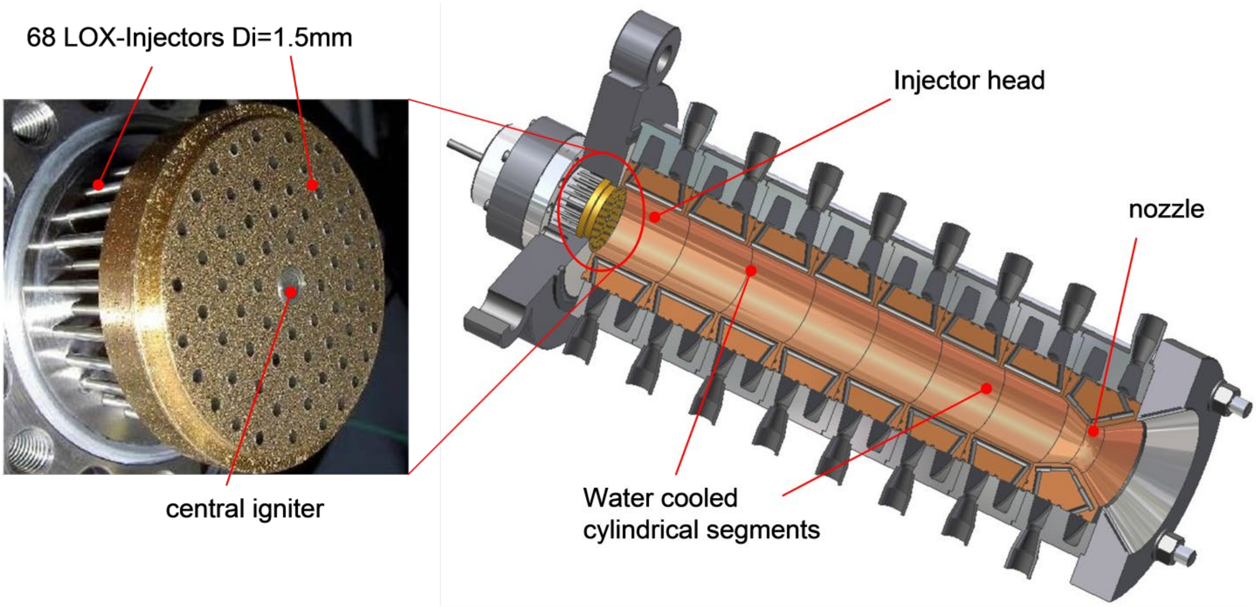


Figure 1: The photo of porous injector head API-68 and the cross-section of sub-scale combustion chamber model “B”.

In the current work the incident heat fluxes to the side walls of the combustion chamber with a porous injector head are studied both experimentally and theoretically. In our previous work [3] we already simulated the flow in the combustion chamber with porous injector head, however it gave us only preliminary results which showed the direction of the further development in numerical simulation.

## 2. Experiments

A segmented, water cooled sub-scale combustor with the porous injector head was designed, manufactured and tested at DLR-Lampoldshausen, see Figures 1 and 2. The combustion chamber operates with LOx/$H_2$ or LOx/$CH_4$ propellant combination in the wide pressure range up to 12 MPa. The hot tests have been done at the European Research and Technology Test Facility P8 (Fig. 2). This test facility operates in a controlled blow-down mode and enables investigations with liquid and gaseous hydrogen and typical rocket engine operating conditions.
The segmented design enables the implementation of various test equipment without the additional expenditure. The combustion chamber has an inner diameter of 50 mm and consists of six cylindrical elements, each of 50 mm length, with a separate cooling supply. The cooling occurs in a row of cylindrical channels. Two collectors in each section provide a uniform mass flow through the all cooling channels. The changeable nozzle throat section makes possible the variation of the contraction ratio ($A_{comb.chamber}/A_{throat}$) from 2 to 8.4. In the current study the nozzle segment with 28 mm throat and corresponding contraction ratio of 3.2 has been used.
Combustion chamber model “B” is used predominantly to study the heat transfer on the hot-side wall and the influence of different design solutions (for example: a new injector head design) on the thermal loads on the combustion chamber walls. Only the calorimetric measurement method has been used in the current study. The wall heat fluxes have been determined using measurements of temperature and pressure at the inlet and the outlet of each section according to the formula:

$$W = \varphi \cdot [h_{out}(T_{out}, P_{out}) - h_{in}(T_{in}, P_{in})], \qquad \textbf{(1)}$$

where $W$ – heat flux to the segment, $\varphi$ – coolant mass flow rate, $h_{out}(T_{out},P_{out})$ – specific enthalpy of water at the outlet of a cylindrical segment as a function of temperature and pressure, $h_{in}(T_{in},P_{in})$ – specific enthalpy of water at the inlet of a segment. An additional temperature sensor measures the surface temperature on the hot-gas side. The summary of the experimental conditions are listed in Tables 1 and 2.

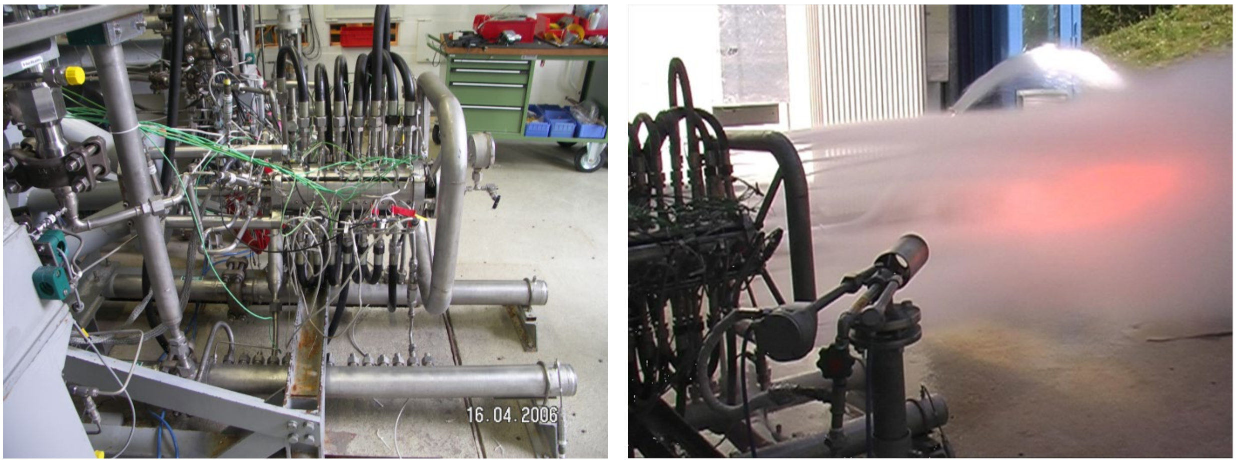


Figure 2: Subscale combustion chamber model "B" at the European Research and Technology Test Facility P8.

Table 1: Conditions of the hot run test.

| | |
|---|---|
| Mass flow rate, $O_2$ | 1.808 kg/s |
| Temperature, $O_2$ | 120 K |
| Mass flow rate, $H_2$ | 0.299 kg/s |
| Temperature, $H_2$ | 100 K |
| ROF | 6 |
| Pressure | ~80 bar |
| Diameter, combustion chamber | 50 mm |
| Diameter, throat | 28 mm |

Table 2: Conditions at the walls of the combustion chamber.

| Segment \ Parameter | Distance to the injector head | Wall temperature | Wall heat flux |
|---|---|---|---|
| S1 | 0–50 mm | 357 K | 0.78 MW/m$^2$ |
| S2 | 50–100 mm | 458 K | 33.5 MW/m$^2$ |
| S3 | 100–150 mm | 552 K | 29.6 MW/m$^2$ |
| S4 | 150–200 mm | 644 K | 29.4 MW/m$^2$ |
| S5 | 200–250 mm | 559 K | 25.1 MW/m$^2$ |
| S6 | 250–300 mm | 647 K | 32.3MW/m$^2$ |
| Nozzle | 300–355 mm | 629 K | 38.3 MW/m$^2$ |

The key feature of the tested combustion chamber is the porous injector head called API-68 ("Advanced Porous Injector"), see Fig. 1. The injector plate is made from sintered bronze. Hydrogen is fed into the combustion chamber through the massive porous plate which consists of sintered bronze beads with the diameter of ~0.6 mm. Liquid oxygen is injected through 68 separate injectors arranged practically uniformly over the porous plate. A single injector is a cylindrical tube with an inner diameter of 1.5 mm. The thickness of the injector tip amounts only 0.25 mm, and fuel and oxidizer get in a direct contact immediately after the injection in contrast to a classical showerhead injector. In the center of the injector plate the outlet of an igniter torch is located.

The combustion chamber with API-68 shows a stable behaviour with the pressure drop between the fuel dome and the chamber below 5% of the mean chamber pressure. The simplicity of this design offers a large potential for the manufacturing cost savings.

## 3. Simulations

The simulations have been performed using commercial CFD code ANSYS CFX [9], which utilizes the finite volume element method (FVEM). The numerical simulations of the flow inside the chamber have been carried out in a three-dimensional computational domain, which represents eight part of the chamber. The domain includes the

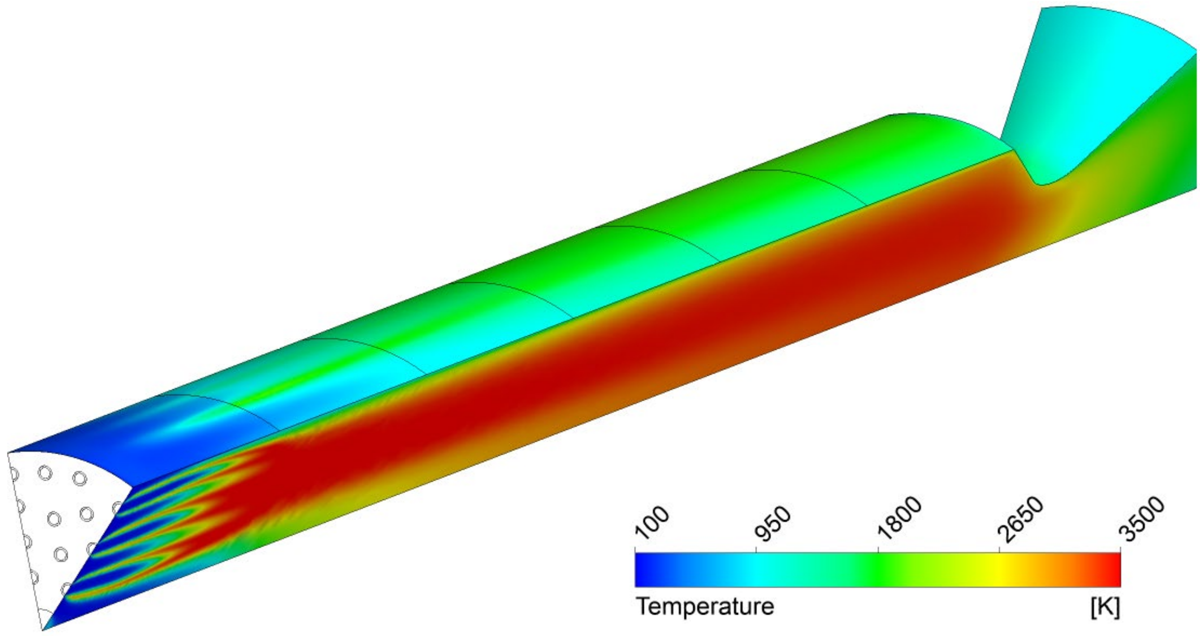


Figure 3: Temperature field simulated by the EDM model at the symmetry plane and at the walls of the combustion chamber.

nozzle, but not the injector head, see Fig. 3. In the numerical domain the turbulent flow of compressible reactive fluid has been simulated. The simulations have been performed on a Dell T7500 workstation with two Intel Xeon E5645 processors.

There are many examples where the flow inside rocket combustion chamber is simulated in a two-dimensional axisymmetric domain (even in the case of the injector head with multiple injectors), for example [7,8]. The substitution of the real geometry by the 2D geometry enables the significant reduction of the computational power which is required for the simulation. Preliminary study [3] showed that in the current case the modelling in 2D domain gives acceptable, but not the very accurate results, that the use of the coarse 3D numerical mesh gives better results than the use of the very fine 2D mesh. The heat flux to the wall is very sensitive to the arrangement of the injectors nearest to the wall. (This conclusion is fully supported by the longstanding experimental experience at DLR-Lampoldshausen.) The semi-rectangular pattern of injectors of the tested injector head API-68 cannot be represented adequately in a 2D axisymmetric geometry. That is why in spite of the significant increase of the size in the numerical mesh the 3D numerical domain has been employed. The arrangement of the injectors has a $90^0$ rotational symmetry plus a reflective symmetry diagonally (Fig. 1), so the geometry of the injector head and the combustion chamber can be fully represented by the sector of $45^0$, see Fig. 3.

The simulations were performed on tetrahedral unstructured meshes with prismatic layers near the walls. The numerical meshes were generated using the computer program ICEM from the package ANSYS CFD. Around twenty different meshes were tested until the final mesh, which gives the mesh independent solution and has a reasonable amount of nodes (1.4 million), has been found. The mesh is refined near the side walls, the injector posts, and the axes of the injectors at the first 50 millimetres from the injector head. The spacing between the nodes varies from 4 µm to 4 mm (the most coarsened mesh is located in the diverging part of the nozzle). The expansion ratio was set to 1.2 for the whole mesh.

The flow in the combustion chamber has been modelled as the stationary solution of the Favre averaged Navier-Stokes equations. The turbulence has been modelled with the help of the Shear-Stress-Transport (SST) model [10] using the standard values of the coefficients and the “automatic” wall function. The transport has been modelled with the turbulent Schmidt number of 0.7 (The value of 0.7 is recommended for high-Reynolds-number jet flows by Yimer et al. [11]). The turbulent Prandtl number has been set to the value of 0.85.

The simulations have been performed using two different combustion models: the Eddy Dissipation Model (EDM) and the Extended Coherent Flame Model (ECFM). (The model called EDM here is indeed far from the original formulation of Magnussen and Hjertager [12] and shares only the concept with the original model, i.e. Eq. (3).) The ECFM model is a combined model employing: the laminar flamelet approach for the mixture composition and the flame surface density model for the reaction progress. In both combustion models the chemical transformations course by global reaction:

$$\tfrac{1}{2}H_2 + O_2 = (1\text{-}y)H_2O + y\cdot X, \qquad \textbf{(2)}$$

where X is other products and depends on the model. Both models use the assumption of thin flame: chemical reactions are infinite fast and chemical transformations are limited by turbulent mixing, so

$$\text{rate} \sim \varepsilon/k, \qquad \textbf{(3)}$$

where $\varepsilon$ is the turbulence eddy dissipation, and $k$ is the turbulent kinetic energy.

The advantages of the EDM are the simplicity and robustness, but to achieve acceptable results the model should be extended especially in the case of rocket combustion (reaction of pure fuel and oxygen at high pressures). At high temperatures (>3000 K) the dissociation of $H_2O$ starts to play a role, in other words (1-y) in Eq. (2) is notably less than 1. To obtain the correct flame temperature in the combustion chamber, which is very important for the heat balance of the combustion chamber and the predictions of the heat fluxes, an external parameter (called “Flame Temperature”) should be introduced in the model. The reaction rate is set to zero when the temperature of reactive mixture reaches the value of “Flame Temperature”, which is precalculated by the use of program NASA CEA [13]. Another external and important parameter in the model is an “Extinction Temperature”. The propellants are injected into the chamber at very low temperature, so it is necessary to set the reaction rate to zero when the temperature of the reactants is obviously below the flammability limit. Here, in contrast to the standard formulation of the EDM model in CFX, the parameters: “Flame Temperature” and “Extinction Temperature” are not constant, but the functions of mixture fraction, which is the mass fraction of element hydrogen in mixture.

The Extended Coherent Flame Model is the most sophisticated turbulent combustion model available in CFX. The ECFM is also based on the assumption of thin flame and Eq. (3). In the ECFM model the species mass fractions are taken from a precalculated “flamelet” library, which associates a given mixture fraction (equivalence ratio) and turbulence intensity with a certain mixture composition. Here the flamelet library was generated using the Peng-Robinson real gas EOS and Burcat’s thermodynamic database [14]. ANSYS CFX has a built-in tool for the generation of flamelet libraries called CFX-RIF. The tool enables the generation of the flamelet library for a $H_2$-$O_2$ mixture using the ideal gas equation of state and the kinetic mechanism of Ó Conaire et al. [15]. The flamelet library generated with the help of CFX-RIF is used here for the comparison. The results obtained with this library named here as “ECFM Ó Conaire”.

The flamelet model requires two variables: a mixture fraction and a mixture fraction variance, while the ECFM needs two more additional variables: a reaction progress and a flame surface density. Reaction progress defines the level of chemical transformations. It enters in the definition of the mixture composition as the blending factor between burnt and unburnt mixtures. The flame surface density is needed for the evaluation of the chemical source (or reaction rate). The resulting model is heavier than the EDM which introduces only two variables: the mass fraction of $H_2$ and the mass fraction of $O_2$. In terms of the computational time the EDM is approximately twice faster, but the ECFM can predict the fractions of intermediates such as H, O, and OH, what may be important in certain cases.

In the combustion chamber temperatures vary from 100 to 3650 K, the pressure is high. Therefore the modelling of the thermodynamic properties of the gas mixture in the combustion chamber is not a simple task. All three major components of the mixture ($H_2$, $O_2$, and $H_2O$) have significant distinctions from ideal gas. Three main non-ideal phenomena have been taken into account: the transition from ortho to para state for hydrogen at low temperatures, the real gas behaviour of oxygen at the low injection temperature, and the dissociation of water at high temperatures. The components of the mixture obey Peng-Robinson real gas equation of state in the model. The enthalpy and the entropy of the components have been defined using NASA polynomials [14]. The dynamic viscosity and thermal conductivity of the mixture and its components have been defined using the empirical formulas according to the recommendations of White [16]. The diffusion coefficients have estimated using the data from Kikoin [17]. The viscosity, the thermal conductivity, and the diffusivity of gases grow with temperature, and the model takes this effect into account. CFX defines the property of multicomponent mixture using a mass averaging, which leads to underestimating the transport coefficients for the mixture of hydrogen with oxygen [18]. For this reason the transport properties of the gas mixture have been modelled separately using the CFX Expression Language. From the original CFX models only the turbulence model and the equation of state were left without modification. The original CFX combustion models have been served only as the framework.

## 4. Results and discussion

The general idea about the flow in the combustion chamber is given in Fig. 3. The flow in the combustion chamber is characterised by the pressure drop within the first 50 mm from the injector face and by the increase of the wall heat flux after the first 50 mm, Fig. 4 and 5. As one can see, the numerical models capture the behaviour of the flow, and moreover the EDM model predicts the results which agree with the experimental data within experimental error.

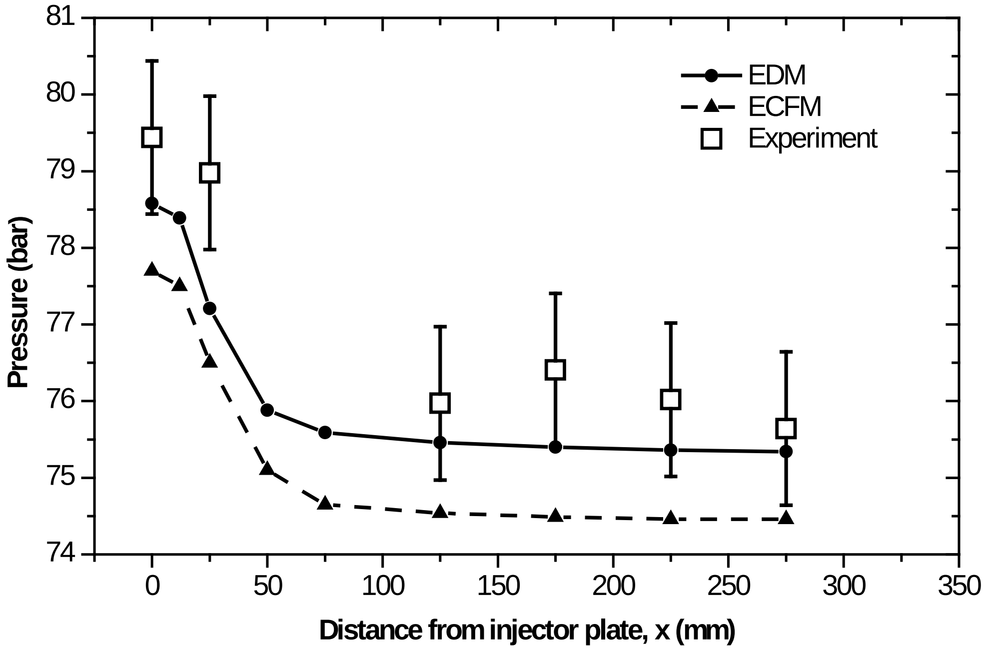


Figure 4: Pressure profile in the combustion chamber. Squares – experiment, solid line and bullets – the EDM model, dash line and triangles – the ECFM model.

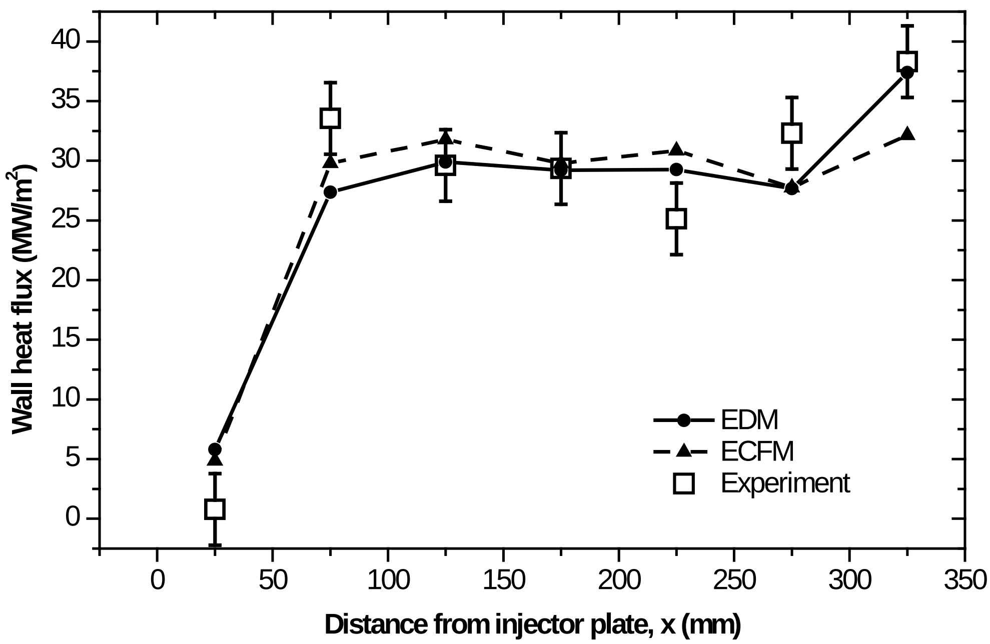


Figure 5: Comparison of the measured and predicted wall heat fluxes. Squares – experiment, solid line and bullets – the EDM model, dash line and triangles – the ECFM model.

The numerical models predict the higher wall heat flux than the measured heat flux in the first section and the lower heat flux in the sixth section. (The first section is next to the injector head, the sixth section is next to the last nozzle section.) Before considering the precision of the numerical models it is necessary to note that the difference between the measured and true values of heat flux may exceed the experimental uncertainties at two locations. The measuring sections are in the thermal contact, by this means the heat may transfer in the longitudinal direction from a hot section to an adjacent colder section. In the hot runs the heat leaks from the most hot nozzle section to the neighbouring sixth section and from the first section to the injector head (the coldest part of the chamber). Thus the true value of the wall heat flux is higher than the measured value in the first section and is lower in the sixth section. At the same time, the numerical model does not take into the processes in the walls of the combustion chamber.

Tucker et al. [19] simulated the flow in a rocket combustion chamber with a single coaxial injector. Comparing the different numerical models the authors concluded that the wall heat flux predictions require time accurate simulations (i.e. URANS or LES) due to the unsteadiness of the flow. In the current work the good agreement with the experimental results has been achieved using RANS (Reynolds-averaged Navier–Stokes equations). In fact the chamber demonstrated the stable operation during the hot runs. In contrast to other combustion chambers, the chamber with a porous injector head does not have stagnation regions which are the sources of flow instabilities.

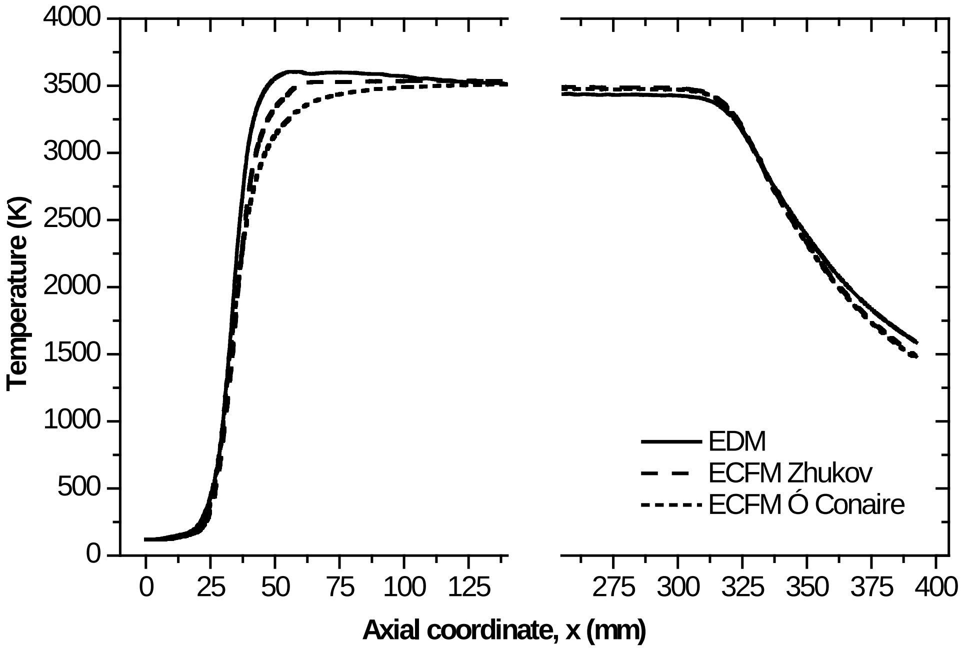


Figure 6: Gas temperature predicted by the different models along the axis of the combustion chamber. Solid line – the EDM model, dash line – the ECFM model, short dash line – the ECFM model with the flamelet library generated by CFX-RIF.

The EDM model predicts the higher wall heat flux (and temperature) in the nozzle than other models, see Fig. 5 and 6. In the nozzle gas expands and the temperature decreases. As soon as the temperature in the nozzle falls below the "Flame Temperature", the reaction occurs again. This slightly compensates the temperature drop in the nozzle. In flamelet models the mixture composition is the function of the mixture fraction (the fraction of fuel in the mixture), but not a function of the temperature. The flamelet models do not assume any reaction behind a flame front. In the real world something similar to the EDM model takes place. The flame temperature is determined by the equilibrium between $H_2O$ and OH. When the temperature of the products decreases, the equilibrium shifts towards the formation of $H_2O$. Since the EDM model is closer to the reality, it gives the results which are closer to the results of the measurements. (The latest 14.5 version of CFX enables the flamelet libraries with different flame temperatures what seems solves the problem of non-adiabatic flames.)

Figures 3, 6 and 7 give the idea about the flame of a single injector. The simulated flame has a spindle shape with the length of 30–50 mm and the diameter of 3–5 mm. The flat temperature minimum in Fig. 7 is a cold oxygen jet.

The graphs in Fig. 6 and 7 give the comparison of the results of the different formulation of the flamelet libraries. The flamelet library generated with the use of CFX-RIF predicts the lower flame temperature in the both axial and radial directions. Pohl et al. [20] did the similar comparison for the flame of coaxial injector and obtained the same results. However, the both flamelet libraries give the same temperature at the flame edge (away from the temperature maximum). Thereby in spite of the different flame temperatures at stoichiometric conditions the both flamelet libraries predict practically the same wall heat fluxes and the pressure in the chamber (the difference between the results obtained with the use of the different flamelet libraries does not exceed indeed the line thickness in Fig. 4 and 5).

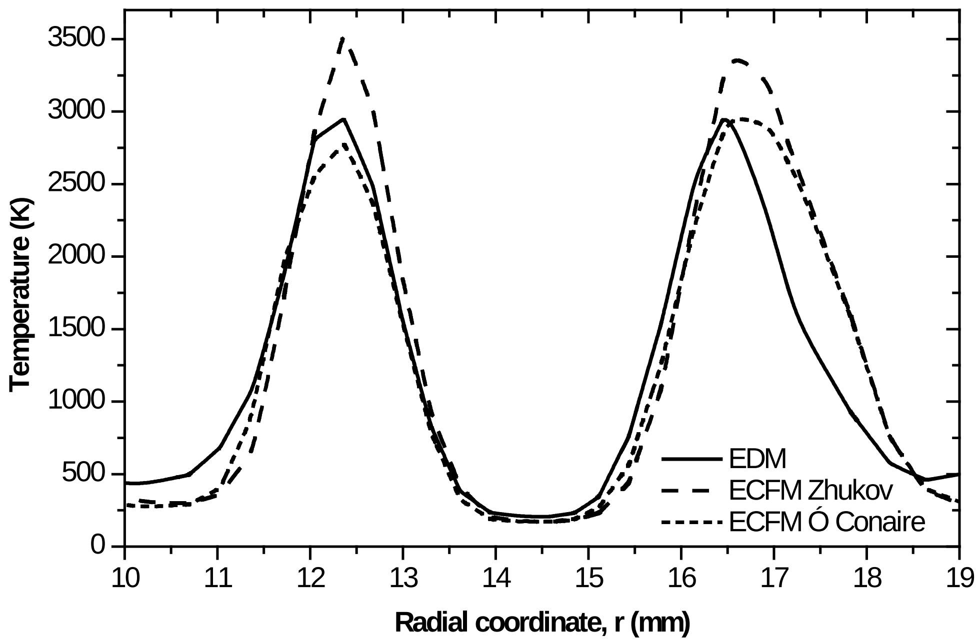


Figure 7: Simulated transverse temperature distribution in the flame of a single injector at an axial location of 20 mm. Solid line – the EDM model, dash line – the ECFM model, short dash line – the ECFM model with the flamelet library generated by CFX-RIF.

The EDM model gives slightly different shape of the flame of a single injector than the ECFM model. The flame is slightly narrower and shorter, see Fig. 6 and 7. The EDM model predicts the higher temperature in the axial direction and the lower temperature in the radial direction. This is again a more natural behaviour of the flame in contrast to other combustion models. In reality the flame has the lower temperature near the injector, where propellants are cold, than further downstream [21]. However, the EDM model overpredicts the flame temperature near the injector head due to the crudity of the model. The model disregards the temperature dependence of the reaction rate and kinetic effects. Nevertheless the EDM model gives better results than the ECFM model which is potentially more precise, but at the current moment is still raw.

The main benefits of the EDM model over the ECFM model are the simplicity and the fact that the parameters of the EDM model have a clear physical meaning. In spite of the apparent crudity of the EDM model it is not primitive. By the EDM model flame is characterised by six parameters in CFX. Three of them have been set as the functions of the local mixture composition here. Hence, the total amount of the coefficients in the used EDM model corresponds to a reaction mechanism with approximately four reactions. In the absence of experimental data the model with the simple and more correct definition give the better results.

## 5. Conclusions

The wall heat fluxes in the combustion chamber with porous injector head API-68 have been measured by the calorimetric method at pressure of 80 bar. The experimental results are characterised by the pressure drop within the first 50 mm from the injector face and by the increase of the wall heat flux after the first 50 mm.

The flow inside the combustion chamber has been simulated using the different combustion models. All tested combustion models agree with the experiment, but the EDM model has the better agreement. The EDM model predicts the pressures and the wall heat fluxes within the experimental error, however, near the injector head and the nozzle the disagreement exceeds the experimental error. The difference between the models and the experiment can be explained by the crudity of the numerical model, but also partially by the longitudinal heat transfer between the adjacent sections of the combustion chamber.

The further development of the combustion models would be a gradual substitution of the parameters estimated theoretically by empirical values. The second step in the development would be a switch from RANS to time accurate turbulence models. The next step in the development of the experimental part could be the measurements with the sections of smaller length and with the thermal insulation between adjacent sections.

## References


[1] Lux J., Suslov D., Haidn O. J., On porous liquid propellant rocket engine injectors, Aerospace Science and Technology, Vol. 12, 2007, pp. 469, 477.

[2] Deeken, J., Suslov, D., Haidn, O.J., Schlechtriem, S., Combustion Efficiency Sensitivity Studies of the API Injector Concept," 49th Aerospace Sciences Meeting including the New Horizons Forum and Aerospace Exposition, AIAA 2011-0793,Orlando, Florida USA,4-7 January, 2011.

[3] Zhukov, V.P., Suslov, D.I., Haidn, O.J., CFD Simulation of Flow in Combustion Chamber with Porous Injector Head and Transpirationally Cooled Walls, Paper id: 29 at 4th European Conference for Aerospace Sciences, Saint Petersburg, Russia, July 4, 2011 – July 8, 2011.

[4] G. C. Sutton, Rocket Propulsion Elements, John Wiley&Sons, 1986/1992/2000.

[5] V.P. Zhukov, O.J. Haidn, Proc. Inst. Mech. Eng. G J. Aerosp. Eng. 227 (5) (2013) 873–881.

[6] Knab O, Preclik D. Test case RCM-3: EADS-ST subscale chamber. 3rd International Workshop Rocket Combustion Modeling, Vernon, France, SNECMA, Villaroche, March, 2006.

[7] Mewes B, Görgen J, Knab O, Frey M. Simulation of the EADS-ST subscale chamber using a dense gas approach. 3rd International Workshop Rocket Combustion Modeling, Vernon, France, SNECMA, Villaroche, March, 2006.

[8] B. Ivančić, H. Riedmann, M. Frey, Validation of Turbulent Combustion Models for 3D-Simulations of Liquid H2/O2 Rocket Combustors, Proceedings of the International Conference on Space propulsion, Bordeaux, France, 7–10 May 2012.

[9] CFX, Software Package, Version 12.1, ANSYS Germany (2009).

[10] F.R. Menter. "Two-Equation Eddy-Viscosity Turbulence Models for Engineering Applications". AIAA Journal. 32(8). 1598–1605. August 1994.

[11] I. Yimer, I. Campbell, L.-Y. Jiang, Estimation of the Turbulent Schmidt Number from Experimental Profiles of Axial Velocity and Concentration for High-Reynolds-Number Jet Flows, Canadian Aeronautics and Space Journal, 2002, 48(3): 195-200, 10.5589/q02-024.

[12] Magnussen, B. F., and Hjertager, B. H., Proc. Combust. Inst. 16 (1976) 719-729.

[13] S. Gordon and B. J. McBride, "Computer Program for Calculation of Complex Chemical Equilibrium Compositions and Applications," NASA Reference Publication 1311 (1996).

[14] Burcat, A.; Third Millennium Ideal Gas and Condensed Phase Thermochemical Database for Combustion. Technion Aerospace Engineering (TAE) Report #867 January 2001, Haifa, Israel.

[15] M. Ó Conaire, H.J. Curran, J.M. Simmie, W.J. Pitz and C.K. Westbrook, Int. J. Chem. Kinet. 36 (2004), pp. 603–622.

[16] White F.M., Viscous Fluid Flow, McGraw-Hill, New York, 1991.

[17] I. Kikoin. Tables of physical values, Atomizdat, Moscow, 1976.

[18] Victor P. Zhukov, "Verification, Validation, and Testing of Kinetic Mechanisms of Hydrogen Combustion in Fluid-Dynamic Computations," ISRN Mechanical Engineering, vol. 2012, Article ID 475607, 11 pages, 2012. doi:10.5402/2012/475607

[19] P.K. Tucker, S. Menon, C.L. Merkle, J.C. Oefelein, and V. Yang, Validation of High-Fidelity CFD Simulations for Rocket Injector Design, AIAA-2008-5226, 44th AIAA/ASME/ SAE /ASEE Joint Propulsion Conference and Exhibit, July 2008.

[20] Pohl S., Poschner, M., Pfitzner M.: "A laminar flamelet model including real gas thermodynamics applied to the CFD-Simulation of LOX/GH2 combustion", 5th European Combustion Meeting, Cardiff, UK, June 28-July 1st 2011 (2011).

[21] M. Habiballah, S. Zurbach, Test Case RCM-3, Mascotte single injector, 3rd Proc. of the 2nd Int. WS on Rocket Combustion Modeling (2001).